Experimental investigations on mixed-mode-loaded cracks

H. A. Richard[1], N.-H. Schirmeisen[2], A. Eberlein[1]

[1] Institute of Applied Mechanics, University of Paderborn, Pohlweg 47-49, 33098 Paderborn, Germany, e-mail: richard@fam.upb.de
[2] Windmoeller & Hoelscher KG, Münsterstr. 50, 49525 Lengerich, Germany, e-mail: nils-henrik.schirmeisen@wuh-group.de

ABSTRACT. *Failure of safety-relevant parts is often caused by a superposition of normal stress as well as plane and anti-plane shear stress. The loading cases of cracks (Mode I, Mode II and Mode III) are generally defined by the stress fields near the crack tip. In contrast to pure Mode I-loaded cracks, whose stress near fields are symmetric, the stress fields near the crack tip of mixed-mode-crack problems are unsymmetrical. Consequently the fracture mechanical treatment of those mixed-mode-loaded cracks is more complicated as of pure Mode I-cracks. This paper deals with experimental investigations of crack growth under spatial mixed-mode-loading. In the following detailed results of fracture and fatigue crack growth experiments and their comparison with existing criteria are presented and discussed.*

INTRODUCTION

In fracture mechanics it is important to understand and analyse the behaviour of mixed-mode fracture, because materials often contain different defects, e.g. pre-cracks, which may have been introduced unintentionally during the manufacturing process. So pre-cracks can have an arbitrary orientation with respect to a general type of loading, which a component of a machine or structure has to carry.

Cracks in structures or materials are generally divided into three fracture modes, which are shown schematically in Figure 1a. The difference of the three fracture modes is the orientation of the local stress filed near the crack tip. A Mode I-loading induces a crack-opening; a Mode II-loading leads to an in-plane fracture of the material, which causes also a crack kinking and a Mode III-loading leads to an anti-plane fracture of the material, which causes a crack twisting (Figure 1b).

Local mixed-mode-loading conditions at cracks occur in combination of the three basic fracture modes. Thereby the cracks grow in a way, that not only an opening, but also a planar deflection and/or a non-planar twisting of the two crack surfaces can be found.

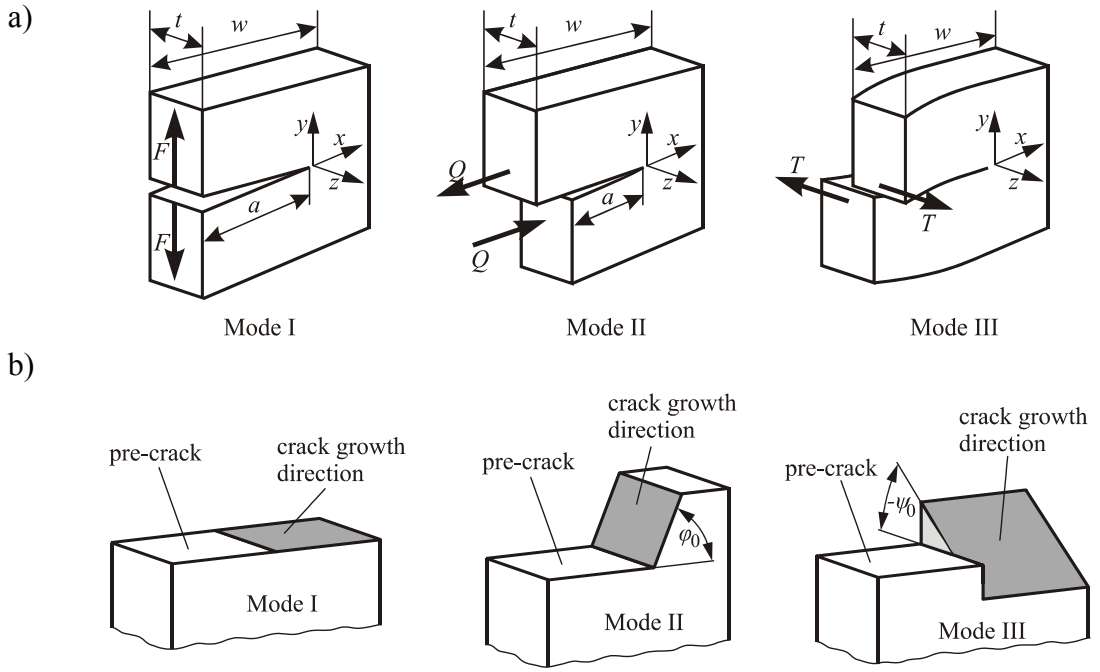

Figure 1. a) Basic fracture modes
b) Principle orientation of the fracture surfaces for basic fracture modes

Therefore the stress field near the crack front is not only defined by the stress intensity factor K_I, but also by K_{II} and K_{III} respectively the comparative stress intensity factor K_V, which can be determined by [1]:

$$K_V = \frac{K_I}{2} + \frac{1}{2} \cdot \sqrt{K_I^2 + 5{,}336 \cdot K_{II}^{\ 2} + 4 \cdot K_{III}^{\ 2}} \tag{1}.$$

According to this the fatigue crack growth is governed by the cyclic stress intensity factors ΔK_I, ΔK_{II} and ΔK_{III} respectively the cyclic comparative stress intensity factor ΔK_V, which can be derived from Eq. 1:

$$\Delta K_V = \frac{\Delta K_I}{2} + \frac{1}{2} \cdot \sqrt{\Delta K_I^2 + 5{,}336 \cdot \Delta K_{II}^{\ 2} + 4 \cdot \Delta K_{III}^{\ 2}} \tag{2}.$$

A crack under spatial-mixed-mode loading is propagable, if ΔK_V exceeds the threshold value ΔK_{th} for Mode I. Unstable crack growth occurs, if K_V (see Eq. 1) reaches the fracture toughness value K_{IC}. Stable and controlled crack growth lies between these two critical values. The complete curves are illustrated in a K_I-K_{II}-K_{III}-diagram (Figure 2a).

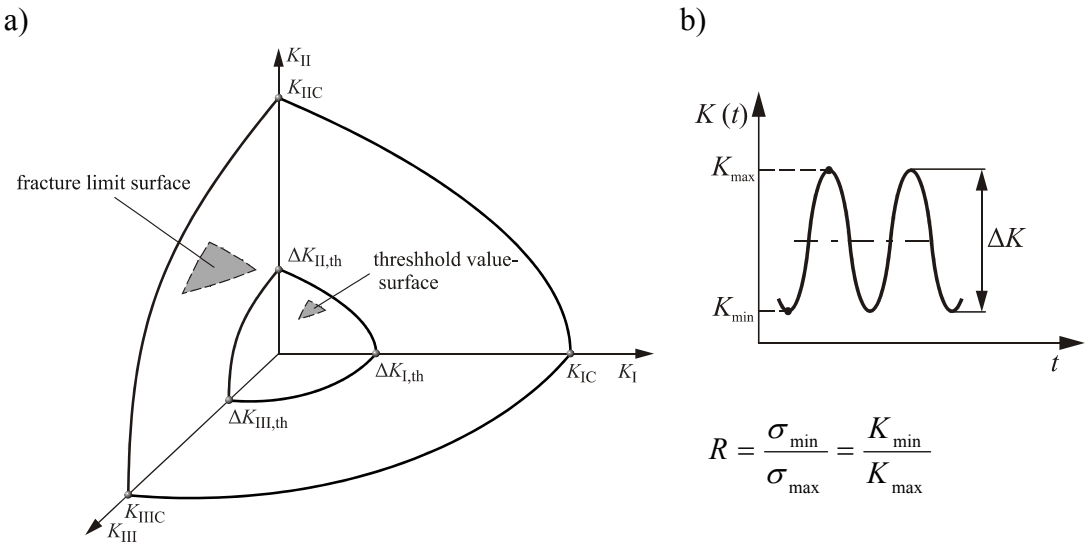

Figure 2. a) K_I-K_{II}-K_{III}-diagram with the range of fatigue crack growth
b) Definition of the cyclic stress intensity factor ΔK and R-ratio

There are numerous hypotheses and concepts for plane- and spatial-mixed-mode problems, which will be described in the following.

EXISTING 2D- AND 3D-MIXED-MODE CRITERIA

For the prediction of the growth of mixed-mode-loaded cracks the determination of comparative stress intensity factors is essential. The transformation of Mode I-, Mode II- and Mode III-stress intensity factor, e. g. by using Eq. 2, into only one cyclic comparative stress intensity factor ΔK_V makes it possible to compare this value with the cyclic fracture toughness value $\Delta K_{IC} = (1\text{-}R)\, K_{IC}$.

Consequently, conclusions could be drawn on crack growth. Furthermore the crack growth direction is required for a complete description of crack growth behaviour. For this purpose some existing hypotheses are mentioned below. All of these hypotheses are based on the near-field-solutions for the stress distribution at the crack front:

$$\sigma_r = \frac{K_I}{4\cdot\sqrt{2\pi\cdot r}}\cdot\left(5\cdot\cos\frac{\varphi}{2}-\cos\frac{3\varphi}{2}\right)-\frac{K_{II}}{4\cdot\sqrt{2\pi\cdot r}}\cdot\left(5\cdot\sin\frac{\varphi}{2}-3\cdot\sin\frac{3\varphi}{2}\right) \quad (3a),$$

$$\sigma_\varphi = \frac{K_I}{4\cdot\sqrt{2\pi\cdot r}}\cdot\left(3\cdot\cos\frac{\varphi}{2}+\cos\frac{3\varphi}{2}\right)-\frac{K_{II}}{4\cdot\sqrt{2\pi\cdot r}}\cdot\left(3\cdot\sin\frac{\varphi}{2}+3\cdot\sin\frac{3\varphi}{2}\right) \quad (3b),$$

$$\tau_{r\varphi} = \frac{K_I}{4\cdot\sqrt{2\pi\cdot r}}\cdot\left(\sin\frac{\varphi}{2}+\sin\frac{3\varphi}{2}\right)+\frac{K_{II}}{4\cdot\sqrt{2\pi\cdot r}}\cdot\left(\cos\frac{\varphi}{2}+3\cdot\cos\frac{3\varphi}{2}\right) \quad (3c),$$

$$\tau_{rz} = \frac{K_{III}}{\sqrt{2\pi\cdot r}}\cdot\sin\frac{\varphi}{2} \quad (3d),$$

$$\tau_{\varphi z} = \frac{K_{III}}{\sqrt{2\pi \cdot r}} \cdot \cos\frac{\varphi}{2} \tag{3e},$$

$$\sigma_z = \nu \cdot (\sigma_r + \sigma_\varphi) = \frac{2\nu}{\sqrt{2\pi \cdot r}} \cdot \left(K_I \cdot \cos\frac{\varphi}{2} - K_{II} \cdot \sin\frac{\varphi}{2} \right) \tag{3f}.$$

2D-Mixed-Mode criteria

For plane-mixed-mode problems in the literature there are many hypotheses [2]. Here in this paper only a few of them are presented.

Criterion by Erdogan and Sih

The crack growth predictions of the maximum tangential stress criterion by Erdogan and Sih [3] are based on the tangential stress σ_φ, Eq. 3b. According to this criterion, the crack growth follows the direction of $\varphi = \varphi_0$ perpendicular to the maximum tangential stress $\sigma_{\varphi,max}$. The crack growth starts radial from the crack tip and becomes unstable as soon as $\sigma_{\varphi,max}$ exceeds the material limit value $\sigma_{\varphi,C}$ – or – if the comparative stress intensity factor K_V, resulting from $\sigma_{\varphi,max}$, exceeds the fracture toughness K_{IC} [2]. The crack deflection angle φ_0 can be obtained by:

$$\left.\frac{\partial \sigma_\varphi}{\partial \varphi}\right|_{\varphi=\varphi_0} = 0 \quad \text{and} \quad \left.\frac{\partial^2 \sigma_\varphi}{\partial \varphi^2}\right|_{\varphi=\varphi_0} < 0$$

Finally the following equation for the crack deflection angle φ_0 results:

$$\varphi_0 = -\arccos\left[\frac{3K_{II}^2 + K_I\sqrt{K_I^2 + 8K_{II}^2}}{K_I^2 + 9K_{II}^2} \right] \tag{4}.$$

The fracture limit surface is given by the maximum comparative stress intensity fractor:

$$K_{V,max} = \sigma_{\varphi,max}\sqrt{2\pi \cdot r} = \cos\left(\frac{\varphi_0}{2}\right) \cdot \left[K_I \cos^2\left(\frac{\varphi_0}{2}\right) - \frac{3}{2} K_{II} \sin(\varphi_0) \right] \tag{5}.$$

2D-criterion by Richard

This criterion was empirically developed by Richard [2, 4]. Here the comparative stress intensity factor K_V is defined by

$$K_V = \frac{K_I}{2} + \frac{1}{2}\sqrt{K_I^2 + 5{,}366 \cdot K_{II}^{\ 2}} = K_{IC} \tag{6}$$

and depends on the stress intensity factors K_I and K_{II}. It is noticeable that unstable crack growth occurs, if K_V exceeds the fracture toughness K_{IC}. This criterion has an excellent approximation of the fracture limit surface of the maximum tangential stress criterion by Erdogan and Sih. The crack kinking angle φ_0 can be determined by

$$\varphi_0 = \mp\left[140° \cdot \frac{|K_{II}|}{|K_I| + |K_{II}|} - 70° \cdot \left(\frac{|K_{II}|}{|K_I| + |K_{II}|}\right)^2\right] \quad (7),$$

whereby for $K_{II} > 0$ the kinking angle $\varphi_0 < 0$ and vice versa, while always $K_I > 0$.

There are some more criteria, e. g. criterion by Nuismer [5] or criterion by Amestoy [6], which are based on the energy release rate and describes the crack growth behaviour for 2D-mixed-mode-loading situations.

3D-Mixed-Mode criteria

Spatial-mixed-mode problems are characterised by the superposition of Mode I-, Mode II- and Mode III-loading. Therefore the stress intensity factors K_I, K_{II} and K_{III} within the scope of linear-elastic fracture mechanics are of importance on the one hand for the estimation of the risk of fracture and on the other hand of the process of the stable crack propagation in a structure.

For non-planar-mixed-mode problems only a few fracture criteria do exist. In the following sections the relevant ones will be described.

Criterion by Sih

The probably best known criterion for the description of three-dimensional-mixed-mode crack problems is the criterion of strain energy density by Sih [7, 8]. It is based on the near-field-equations (Eq. 3a-3f) and on the elastic energy density for spatial-mixed-mode problems. Beginning from the crack tip the crack grows radial in the direction of the minimal energy density factor S_{min} and becomes unstable as soon as S_{min} exceeds a critical material value S_C [7, 8].

Criterion by Pook

Another criterion for spatial crack growth was proposed by Pook [9-11]. In order to determine the crack growth direction and a comparative stress intensity factor, first of all he calculates a plane comparative stress intensity factor $K_{V,I,II}$ with the following equation:

$$K_{V,I,II} = \frac{0{,}83 K_I \cdot \sqrt{0{,}4489 K_I^2 + 3 K_{II}^2}}{1{,}5} \quad (10).$$

Afterwards he determines by using the $K_{V,I,II}$ and K_{III} a spatial comparative stress intensity factor $K_{V,I,II,III}$

$$K_{V,I,II,III} = \frac{K_{V,I,II} \cdot (1+2\nu) + \sqrt{K_{V,I,II}^2 \cdot (1-2\nu)^2 + 4K_{III}^2}}{1{,}5} = K_{IC} \tag{11}.$$

In order to be able to make conclusions about the occurence of unstable crack growth the $K_{V,I,II,III}$ can be compared with the fracture toughness K_{IC}. The crack kinking angle φ_0 can be obtained by:

$$K_I \sin\varphi_0 = K_{II}(3\cos\varphi_0 - 1) \tag{12}$$

and the crack twisting angle ψ_0 by:

$$\tan 2\psi_0 = \frac{2K_{III}}{K_{V,I,II}(1-2\nu)} \tag{13}.$$

The crack deflection angles (see Figure 1b) results in a range of [-70.5°,+70.5°] for φ_0 and [-45°,+45°] for ψ_0.

Criterion by Schöllmann et al.

The σ_1'-criterion by Schöllmann et al. [12, 13] is based on the assumption that crack growth develops perpendicularly to the direction of σ_1' (Figure 3). For the determination of this special maximum principal stress the near-field equations (Eq. 3a-3f) are used.

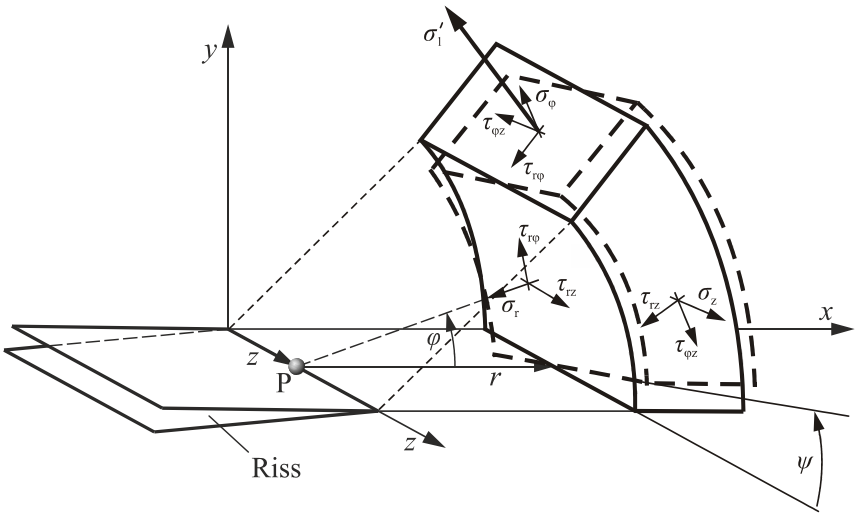

Figure 3. Cylindrical coordinate system and stress components at a 3D-crack front

σ_1' depends on the near-field-stresses σ_φ, σ_z and $\tau_{\varphi z}$ as follows:

$$\sigma_1' = \frac{\sigma_\varphi + \sigma_z}{2} + \frac{1}{2}\sqrt{(\sigma_\varphi - \sigma_z)^2 + 4\tau_{\varphi z}} \tag{14}.$$

According to this criterion the crack kinking angle φ_0 occurs as soon as σ_1' reaches its maximum value. Therefor Eq. 14 has to fulfil the following conditions:

$$\left.\frac{\partial \sigma_1'}{\partial \varphi}\right|_{\varphi=\varphi_0} = 0 \quad \text{and} \quad \left.\frac{\partial^2 \sigma_1'}{\partial \varphi^2}\right|_{\varphi=\varphi_0} < 0$$

After substituting the near-field equations (Eq. 3a-3f) into Eq. 14, considering σ_z is zero and differentiating partially with respect to φ_0, the following equation can be found for φ_0:

$$\begin{aligned} &-6K_I \tan\left(\frac{\varphi_0}{2}\right) - K_{II}\left(6 - 12\tan^2\left(\frac{\varphi_0}{2}\right)\right) + \left\{\left[4K_I - 12K_{II}\tan\left(\frac{\varphi_0}{2}\right)\right]\cdot\right. \\ &\cdot\left[-6K_I \tan\left(\frac{\varphi_0}{2}\right) - K_{II}\left(6 - 12\tan^2\left(\frac{\varphi_0}{2}\right)\right)\right] - 32K_{III}^2 \tan\left(\frac{\varphi_0}{2}\right)\cdot \\ &\left.\cdot\left(1 + \tan^2\left(\frac{\varphi_0}{2}\right)\right)^2\right\}\cdot\left\{\left[4K_I - 12K_{II}\tan\left(\frac{\varphi_0}{2}\right)\right]^2 + 64K_{III}^2\left(1 + \tan^2\left(\frac{\varphi_0}{2}\right)\right)^2\right\}^{-1/2} = 0 \end{aligned} \tag{15}.$$

In order to understand the complete crack growth behaviour for spatial-mixed-mode case a specification of the twisting angle ψ_0 is necessary. The twisting angle is defined by the direction of σ_1' and can be formulated as follows:

$$\psi_0 = \frac{1}{2}\arctan\left(\frac{2\tau_{\varphi z}(\varphi_0)}{\sigma_\varphi(\varphi_0) - \sigma_z(\varphi_0)}\right) \tag{16}.$$

A comparative stress intensity factor $K_{V,max}$ can be established out of Eq. 14 by using:

$$K_{V,max} = \sigma_{1,max}'\sqrt{2\pi \cdot r} \tag{17}$$

with $\varphi = \varphi_0$ the $K_{V,max}$ results from:

$$K_{\mathrm{V,max}} = \frac{1}{2}\cos\left(\frac{\varphi_0}{2}\right)\cdot\left\{\begin{array}{l} K_{\mathrm{I}}\cos^2\left(\frac{\varphi_0}{2}\right) - \frac{3}{2}K_{\mathrm{II}}\sin(\varphi_0) \\ + \sqrt{\left[K_{\mathrm{I}}\cos^2\left(\frac{\varphi_0}{2}\right) - \frac{3}{2}K_{\mathrm{II}}\sin(\varphi_0)\right]^2 + 4K_{\mathrm{III}}^2} \end{array}\right\} \tag{18}.$$

For completeness another one criterion has to be mentioned here. The MTU-criterion by Dhondt [14] is very similar to the criterion by Schöllmann et al., because it has the same assumptions.

3D-criterion by RICHARD
The basis for this criterion is the following approach:

$$\left(\frac{K_{\mathrm{I}}}{K_{\mathrm{IC}}}\right)^{\mathrm{u}} + \left(\frac{K_{\mathrm{II}}}{K_{\mathrm{IIC}}}\right)^{\mathrm{v}} + \left(\frac{K_{\mathrm{III}}}{K_{\mathrm{IIIC}}}\right)^{\mathrm{w}} = 1 \tag{19}.$$

With $u = 1$ and $v = w = 2$ a cyclic comparative stress intensity factor can be defined in order to reasonably describe fatigue crack growth:

$$\Delta K_{\mathrm{V}} = \frac{\Delta K_{\mathrm{I}}}{2} + \frac{1}{2}\sqrt{\Delta K_{\mathrm{I}}^2 + 5{,}336\cdot\Delta K_{\mathrm{II}}{}^2 + 4\cdot\Delta K_{\mathrm{III}}{}^2} \tag{20}.$$

Fatigue crack growth starts, if ΔK_{V} exceeds the threshold value of fatigue crack growth ΔK_{th}. Crack growth becomes unstable, if the fracture toughness K_{IC} is reached. This criterion by Richard is a good approximation to the criterion by Schöllmann et al. For the determination of the kinking angle φ_0 and the twisting angle ψ_0 simple approximation functions are given by [1]

$$\varphi_0 = \mp\left[140°\cdot\frac{|K_{\mathrm{II}}|}{|K_{\mathrm{I}}|+|K_{\mathrm{II}}|+|K_{\mathrm{III}}|} - 70°\cdot\left(\frac{|K_{\mathrm{II}}|}{|K_{\mathrm{I}}|+|K_{\mathrm{II}}|+|K_{\mathrm{III}}|}\right)^2\right] \tag{21},$$

$$\psi_0 = \mp\left[78°\cdot\frac{|K_{\mathrm{II}}|}{|K_{\mathrm{I}}|+|K_{\mathrm{II}}|+|K_{\mathrm{III}}|} - 33°\cdot\left(\frac{|K_{\mathrm{II}}|}{|K_{\mathrm{I}}|+|K_{\mathrm{II}}|+|K_{\mathrm{III}}|}\right)^2\right] \tag{22}.$$

For $K_{\mathrm{I}} \geq 0$ and $K_{\mathrm{II}} < 0$ is $\varphi_0 > 0$ and for $K_{\mathrm{II}} > 0$ is $\varphi_0 < 0$. Furthermore, for $K_{\mathrm{I}} \geq 0$ and $K_{\mathrm{III}} < 0$ is $\psi_0 > 0$ and for $K_{\mathrm{III}} > 0$ is $\psi_0 < 0$.

EXPERIMENTAL INVESTIGATIONS ON 2D-MIXED-MODE-CRACKS

In the past several specimen types for 2D-mixed-mode problems have been proposed [2, 15]. Among others, the CTS-specimen together with its loading device [16, 17] has proven its applicability. Therefore only the CTS-specimen will be discussed in the following.

The loading device (Figure 4) allows applying pure Mode I-, pure Mode II- as well as almost every 2D-mixed-mode-loading combination to the CTS-specimen by using just a uniaxial tension testing machine. For the purpose of varying the mixed-mode-loading only the loading angle α has to be changed.

Depending on the mixed-mode-portion the crack grows into a new direction, i. e. the crack kinks under a specific angle φ_0 (see Eq. 7). Some fractured CTS-specimens with an increasing K_{II}/K_I-portion are shown in [18].

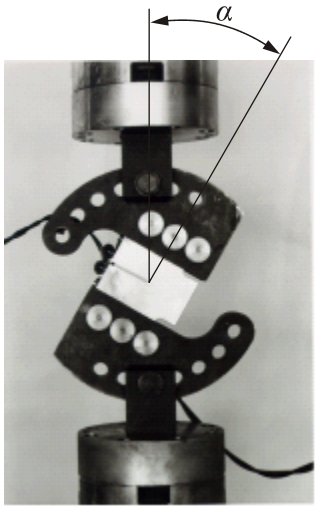

Figure 4. Loading device and the adjustment of the loading angle α

EXPERIMENTAL INVESTIGATIONS ON 3D-MIXED-MODE-CRACKS

For experimental investigations of three-dimensional crack growth and fatigue for spatial-mixed-mode loading some types of specimens are available [2, 3, 19]. But in fact only view of these specimens covers the full range of all basic fracture modes or all combinations thereof.

Due to their importance for the researches of mixed-mode-loaded crack problems, in this paper the AFM-specimen and the CTSR-specimen with their corresponding loading devices (cf. Figs. 5 and 7) are described in more detail.

AFM (All-Fracture-Mode)-specimen and loading device

The AFM-specimen, developed by Richard, enables the investigation of spatial-mixed-mode problems in arbitrary combination by using a simple uniaxial testing machine [20].

Some experiments under static load [21] had proven the applicability of this loading device. Due to its high weight and high deformation only low test frequency for fatigue is possible. Consequently this fact leads to very high duration of experiments.

Referring to this concept by Richard a new specimen, so-called CTSR-specimen, with the corresponding loading device was developed, which is discussed in more detail below.

Figure 5. Loading device for AFM-specimen

CTSR (Compact-Tension-Shear-Rotation)-specimen and loading device

In the last few years an advanced AFM-specimen, so-called CTSR (Compact Tension Shear Rotation) -specimen (Figure 6) for cycling loading was developed [22]. The appropriate loading device is shown in Figure 7. This new specimen and corresponding loading device enables any combination of mixed-mode loading including pure Mode I-, pure Mode II- and pure Mode III-loading. Because of the holes, which are installed circularly in 15°-steps at a bolt circle around the specimen, it is possible to generate any ratio of Mode I to Mode II/Mode III (Figure 7).

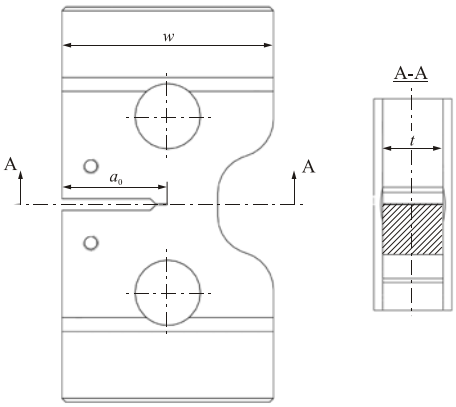

Figure 6. CTSR-specimen

By rotating the so-called turret inside the loading device the ratio of Mode II- or Mode III-load is set (Figure 8).

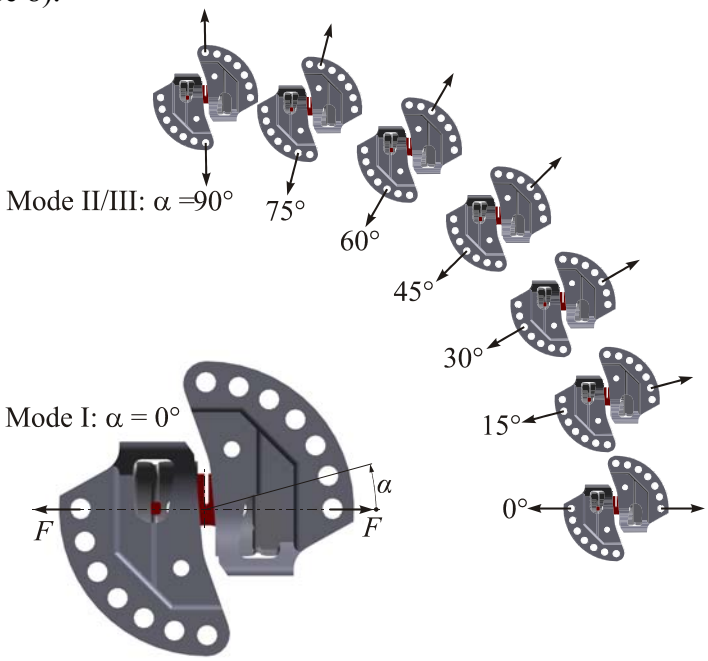

Figure 7. Loading device: Adjustment of the ratio of Mode I to Mode II/Mode III

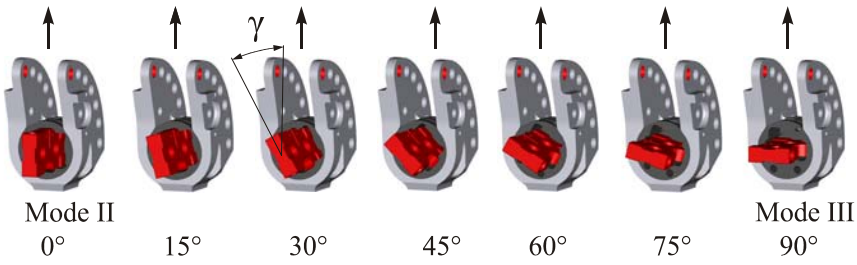

Figure 8. Loading device: Adjustment of Mode II- and Mode III- ratio

The angles α and γ can be adjusted by 15°-steps in the range from 0° to 90°. Whereby the load line of action always passes through the centre of the specimen.

In the following section results of fracture and fatigue crack growth experiments and also comparisons with existing criteria are shown and discussed.

RESULTS OF 3D-MIXED-MODE EXPERIMENTS ON CTSR-SPECIMENS

First of all experiments on PMMA have been performed, in order to determine the fracture limit surface. Another series of experiments were done, in order to determine the threshold-value surface (cf. Fig. 2a) for the aluminium alloy Al7075-T651. Some resulting fractured surfaces of fatigue experiments are presented in Figure 9.

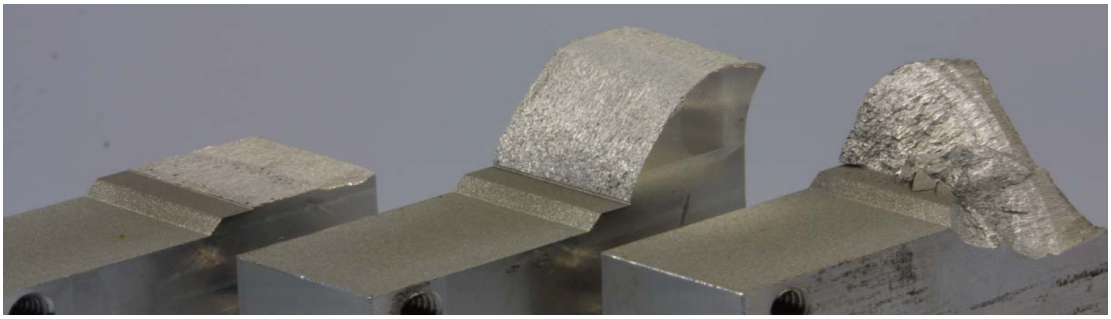

Figure 9. Mode I-, Mode II- and Mode III-fractured surface of Al7075-T651 (form left to right)

The direction of crack propagation changes depending on the loading situation (look at Fig. 1b). At a Mode I-loading the crack grows in the direction of the initial crack front; at a Mode II-loading a clear crack kinking is noticed and Mode III-loading leads to crack twisting and creates facets.

Comparison of the results with existing criteria

The points in Figure 10 are measured on CTSR-specimens (see Figure 6) the fracture toughness values for PMMA. By comparison with the 3D-criterion by Richard a significant variation of the fracture toughness values determined by Mode III-loading is noticeable. The resulting facture toughness values for pure Mode III-loading K_{IIIC} are around factor 2.7 above the hypotheses by Richard. A comparison with other criteria mentioned in this paper show the same results.

Furthermore it is visible, that the less the Mode III-ratio the better the congruence with the predictions of the hypotheses. As soon as there is no Mode III-loading the measured values are very close by the criterion by Richard. All in this paper investigated criteria are conservative, so they could be used for engineering calculations.

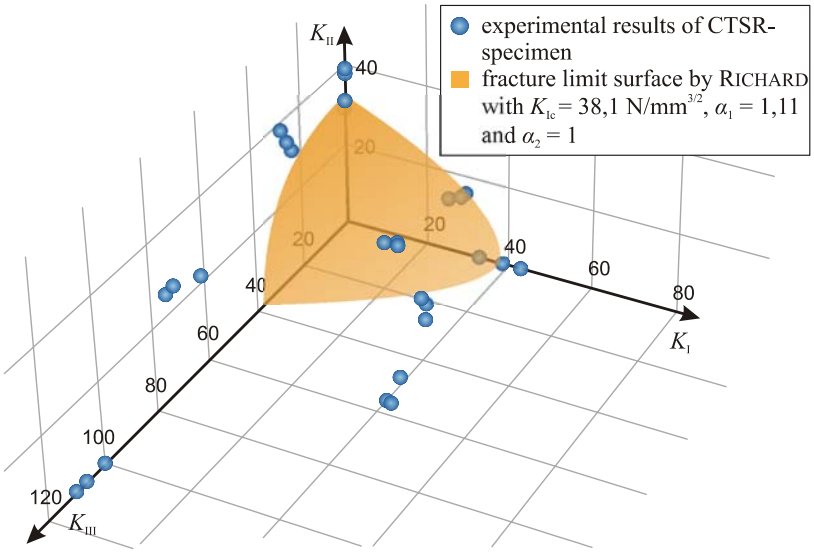

Figure 10. Comparison of experimental results with 3D-criterion by Richard

In addition, the comparison of measured threshold values of Al7075-T651 with the threshold value surface of the criterion by Richard also depicts a significant variation of threshold values for Mode III-loading $\Delta K_{III,th}$ (Figure 11). Here the resulting threshold values for pure Mode III-loading $\Delta K_{III,th}$ are around factor 2.2 above the hypotheses by Richard (see Eq. 20). The threshold values for all in this paper investigated criterions are on the safe side, so they could be used for fracture mechanical calculations.

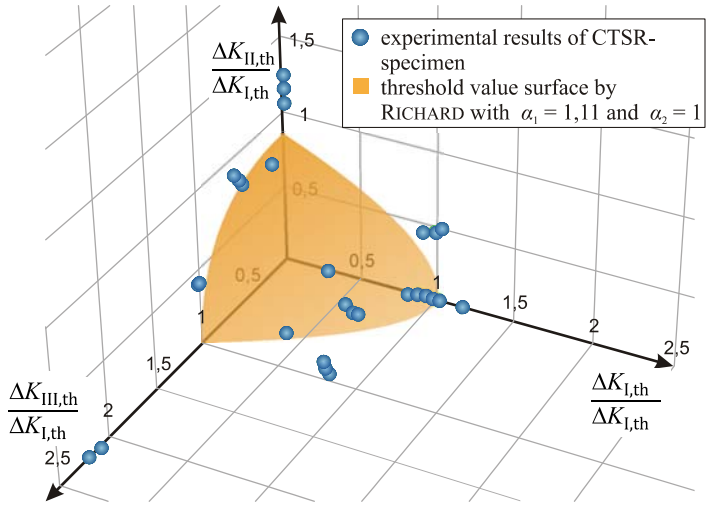

Figure 11. Comparison of threshold value results with 3D-criterion by Richard

Moreover, the crack kinking and crack twisting were investigated. Therefor the fractured surfaces of the specimens (Figure 12a) were digitalised by using an optical 3D-scanner. The result of such a digitalisation is presented in Figure 12b.

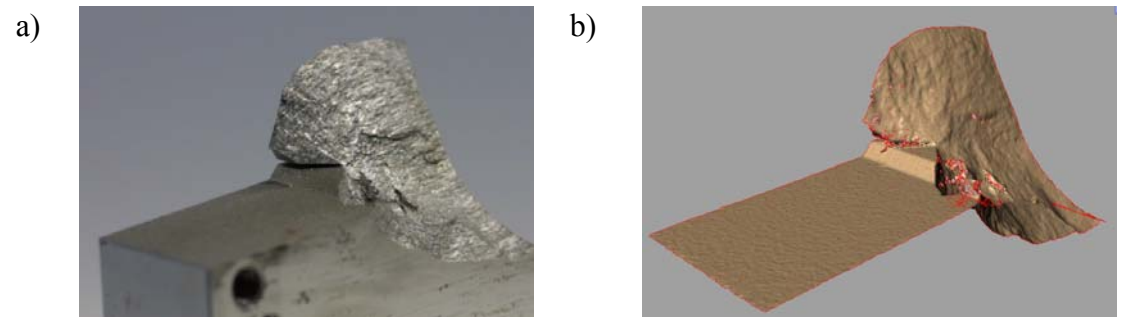

Figure 12. a) Real fractured surface
b) Digitalised fractured surface

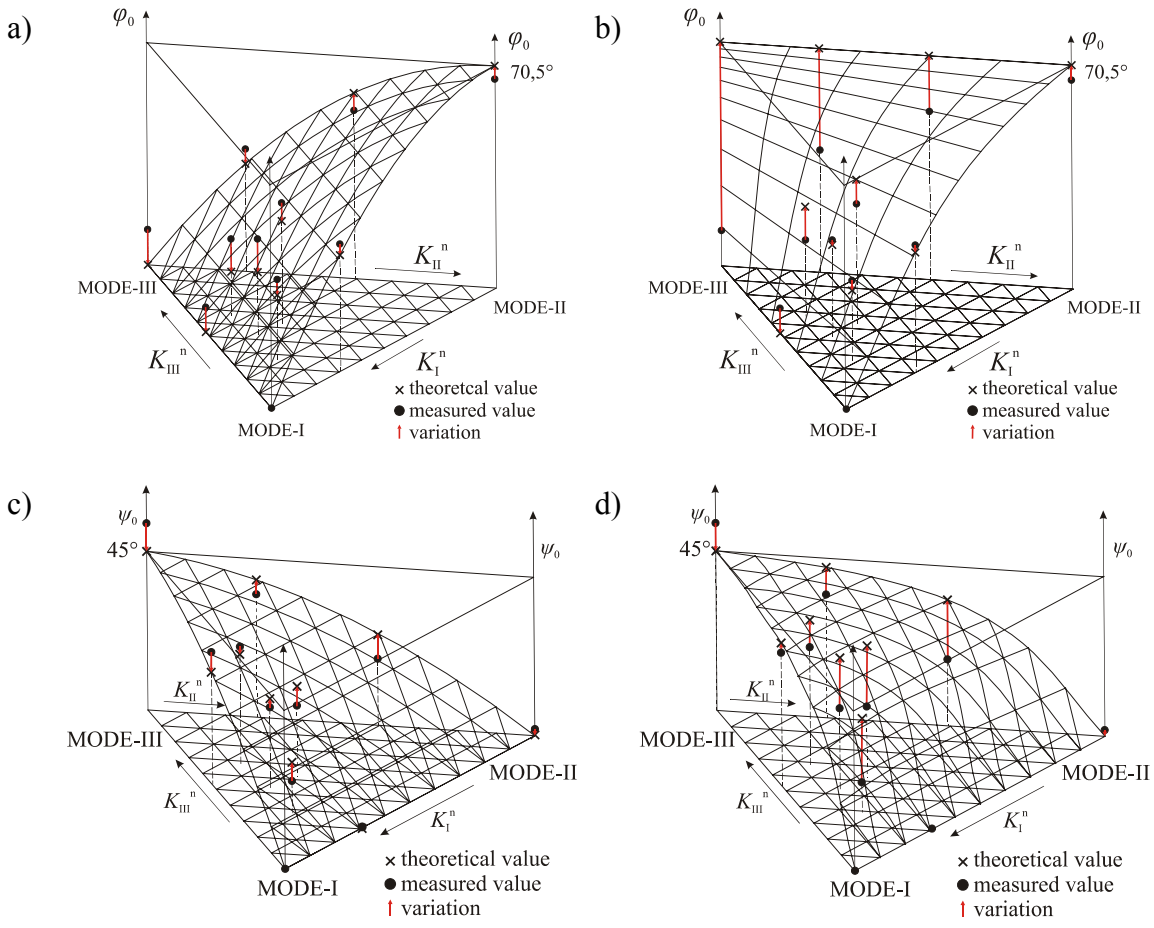

Figure 13. a) Comparison of kinking angle with criterion by Richard
b) Comparison of kinking angle with criterion by Pook
c) Comparison of twisting angle with criterion by Richard
d) Comparison of twisting angle with criterion by Pook

With a CAD-software the data from the optical 3D-scanner further were processed and an approximation area near the initial crack front was defined in order to determine

kinking and twisting angles φ_0 and ψ_0. Then the angle values were compared with the criteria to prove the reliability of their predictions.

The comparison between measured crack deflection angles and the predictions of criteria (look at Figure 13) exhibits that measured crack kinking angle φ_0 coincides very well with the predictions of the criterion by Richard (Figure 13a) as well as of criterion by Schöllmann et al. and criterion by Dhondt. The average deviation for the crack kinking angle φ_0 is ca. 7°. Maximum deviation can be found at pure Mode III-loading.

The criterion by Pook disregards that fact. Consequently the real kinking angle deviates considerably from its predictions (Figure 13b).

A similar result exhibits the evaluation of the crack twisting angle ψ_0. The results show a very well coincidence of the real crack twisting angle ψ_0 with the predictions of the criterion by Richard as well as of the criterion by Schöllmann et al., as mentioned above (Figure 13c). The greatest deviations from the real twisting angle one finds at the predictions of the criteria by Pook (Figure 13d) and by Dhondt.

CONCLUSION

In conclusion, it can be said that, the new developed CTSR-specimen, which was presented here, is suitable for experimental investigations on spatial-mixed-mode loading.

On consideration of fatigue tests the results show obviously higher fracture toughness values and threshold values for high Mode III-loading ratios than by existing criteria theoretically expected. Predictions of all criteria are on the conservative side. Here the criteria by Richard and by Schöllmann et al. indicate the most exactly predictions.

Good predictions regarding both crack deflection angles are predicted by the criteria by Richard, by Schöllmann et al. and also by Dhondt. Due to their good exactness of predictions of the fatigue crack growth behaviour, these criteria should be implemented in numerical calculation programs.

REFERENCES

1. Richard, H.A., Fulland, M., Sander, M. (2005). *FFEMS* **28**, 3-12.
2. Richard, H.A. (1985) *Bruchvorhersage bei überlagerter Normal- und Schubbeanspruchung von Rissen*, VDI-Verlag, Düsseldorf.
3. Erdogan, F., Sih, G.C. (1963) *J. Basic Engng*. **85**, 519-525
4. Richard, H.A. (1987) In: *Structural failure, product liability and technical insurance,* Rossmanith (Ed.), Inderscience Enterprises Ltd., Genf.
5. Nuismer, R.J. (1975) *Int. J. Frac* **11**, 245-250.
6. Amestoy, M., Bui, H.D., Dang Van K. (1980) In: *Advances in Fracture research,* pp. 107-113, Francois, D. et al. (Eds.), Oxford.

7. Sih, G.C. (1974) *Int. J. Frac* **10**, 305-321.
8. Sih, G.C. (1990). *Mechanics of fracture initiation and propagation,* Kluwer Academic publishers, Dodrecht, Netherlands.
9. Pook, L.P. (1980). In: *Fracture and Fatigue: Elasto-Plasticity, Thin Sheet and Micromechanism Problems,* pp. 143-153, Radon, J.C. (Ed.) Pergamon Press, Oxford.
10. Pook, L.P. (1985). *Multiaxial Fatigues,* pp. 249-263 In: Miller, K.J., Brown, M.W. (Eds.), ASTM STP853, American Society for Testing and Materials, Philadelphia.
11. Pook, L.P. (2000). *Linear elastic fracture Mechanics for engineers: theory and application.* WIT press, Southampton.
12. Schöllmann, M., Kullmer, G., Fulland, M., Richard, H.A, (2001), *Proc. of 6th Int. Conf. of Biaxial/Multiaxial Fatigue & Fracture*, Vol. **2**, 589-596.
13. Schöllmann, M., Richard, H.A., Kullmer, G. and Fulland, M. (2002) *Int. J. Frac.* **117**, 129-141.
14. Dhondt, G. (2003) In: *Key Engineering Materials* **251-252**, 209-214.
15. Richard, H.A (1989), In: *Biaxial and Multiaxial Fatigue*, pp. 217-229, Brown, M.W., Miller, K.J (Eds.), Mechanical Engineering Publications, London.
16. Richard, H.A., Benitz, K., (1983) *Int. J. Frac.* **22**, R55/R58.
17. Richard, H.A. (1984) In: *Advances in Fracture Research*, pp. 3337-3344, Valluri, S.R. et al. (Eds.), Pergamon Press, Oxford.
18. Richard, H.A, Schöllmann, M., Fulland, M., Sander, M. (2001), *Proc. of 6th Int. Conf. of Biaxial/Multiaxial Fatigue & Fracture*, Vol. **2**, 623-630.
19. Davenport, J.C.W. and Smith, D.J. (1993). *Fat. Fract. Engng. Mater. Struct.*, 16, 10, 1125.
20. Richard, H.A. (1983) *Praxisgerechte Simulation des Werkstoff- und Bauteilverhaltens durch überlagerte Zug-, ebene Schub- und nichtebene Schubbelastung von Proben*, VDI-Verlag, Düsseldorf, 269-274.
21. Richard, H.A., Kuna, M. (1990) *Eng. Frac. Mech.*, Vol. **35**, No. 6, pp. 949-960.
22. Schirmeisen, N.-H., Richard, H.A. (2009) In: *DVM-Bericht 241*, pp. 211-220, Deutscher Verband für Materialforschung und –prüfung e.V., Berlin.